Journal of Plant Physiology **165** (2008) 1300—1312

Available online at www.sciencedirect.com

ScienceDirect

JOURNAL OF PLANT PHYSIOLOGY

www.elsevier.de/jplph

Solanum lycopersicon Mill. and *Nicotiana benthamiana* L. under high light show distinct responses to anti-oxidative stress

Luísa C. Carvalho, Sónia Santos, B. Jorge Vilela, Sara Amâncio*

DBEB/CBAA, Instituto Superior de Agronomia, Universidade Técnica de Lisboa, Tapada da Ajuda, 1349-017 Lisboa, Portugal

Received 29 September 2006; received in revised form 16 April 2007; accepted 18 April 2007

KEYWORDS
Asc–glut cycle;
Hydrogen peroxide;
Photooxidative stress;
Real-time PCR;
Superoxide ion

Summary

Two experimentally important species, *Solanum lycopersicon* Mill. and *Nicotiana benthamiana* L., were propagated *in vitro* under low light (50 μmol m^{-2} s^{-1}) and transferred to HL (200 μmol m^{-2} s^{-1}) under a protocol previously developed for grapevine and chestnut. Compared with photooxidative stress parameters already tested in those species, imaging of hydrogen peroxide and superoxide revealed an accumulation on d2–3 and d6 in *S. lycopersicon* and d1–2 and d5–7 in *N. benthamiana*. SOD, CAT and APX activities matched ROS accumulation. The expression of the respective transcripts showed a significant increase on d1 in *S. lycopersicon* while in *N. benthamiana* a bimodal pattern was found, with peaks on d2 and d7. These results, together with the relative timing of root expansion and new leaf emergence, indicate that these two apparently similar species display different strategies when responding to light stress, evidencing further the uniqueness of the response of each species. The behaviour of *N. benthamiana* falls closely into the pattern already reported for wood species including grapevine.

Introduction

In vitro plantlets are developed under low light, on media containing ample sugar and nutrients to allow for heterotrophic growth, in closed vessels under a high level of humidity. These conditions set the stage for down-regulation of photosynthesis, either due to a lack of CO_2 in the culture vessels or from the feedback inhibition of Calvin cycle enzymes by the sucrose supply to the media. Nevertheless, *in vitro* plantlets can develop a functional photosynthetic apparatus with the capacity for attaining measurable photosynthetic rates (van Huylenbroeck et al., 2000; Carvalho

*Corresponding author. Tel.: +351 21 3653418; fax: +351 21 3653238.
E-mail address: samport@isa.utl.pt (S. Amâncio).

0176-1617/$ - see front matter © 2007 Elsevier GmbH. All rights reserved.
doi:10.1016/j.jplph.2007.04.009

et al., 2001). However, most species show a culture-induced phenotype, with specific physiological and anatomical characteristics, which impairs their survival when transferred directly to the greenhouse or field conditions (for a review, see Desjardins, 1995; Kozai and Smith, 1995).

Considerable efforts have been directed to optimize the setting for acclimatization of micropropagated plants to *ex vitro* environments, although each species seems to behave in a particular way and a protocol that has proven to be ideal for one species can prove disastrous for another. Nevertheless, there are several common aspects of acclimatization, such as the tight control of relative humidity (RH) and light intensity during this period. It has been reported previously that plantlets transferred to *ex vitro* under irradiances higher than *in vitro* show photoinhibition symptoms (van Huylenbroeck et al., 2000; Carvalho et al., 2001) as a consequence of the production of reactive oxygen species (ROS) caused by excess photon energy, although plants can recover by activating their anti-oxidant system and develop new structures (Carvalho et al., 2006).

Besides the well-described harmful effects of ROS in plant cells, they also play important roles in defence mechanisms against biotic and abiotic stress and in the regulation of biological processes associated with development, e.g. the cell cycle, programmed cell death and hormone signalling (Mullineaux and Karpinsky, 2002; Mittler, 2002; Appel and Hirt, 2004; Kwak et al., 2006; Torres et al., 2006). The use of ROS as signalling molecules by plant cells suggests that, during the course of evolution, plants were able to achieve a high degree of control over ROS toxicity, enabling their function as signalling molecules (Mittler et al., 2004; Kwak et al., 2006). However, controlling ROS toxicity while allowing hydrogen peroxide (H_2O_2) or superoxide ($O_2^{\cdot-}$) to act as signalling molecules appears to require a large gene network composed of at least 152 genes in *Arabidopsis* (Mittler et al., 2004). Major ROS-scavenging enzymes of plants include superoxide dismutase (SOD), ascorbate peroxidase (APX) and catalase (CAT). Together with the antioxidants ascorbic acid and glutathione (Noctor and Foyer, 1998), these enzymes provide cells with efficient machinery for detoxifying $O_2^{\cdot-}$ and H_2O_2, namely through the asc–glut cycle. The cellular pools of ascorbic acid and glutathione are maintained in their reduced state by the NAD(P)H-dependent enzymes monodehydroascorbate reductase (MDHAR), dehydroascorbate reductase (DHAR) and glutathione reductase (GR). Although DHARs are able to reduce dehydroascorbic acid, many other enzymes in plants can catalyse this reaction with different efficiencies (Chew et al., 2003). In addition, monodehydroascorbate radicals can be reduced via ferredoxin using electrons diverted from the photosynthetic apparatus, in chloroplast water–water cycle (Asada, 1999).

In previous work, we established experimental protocols for the perennial wood plants grapevine (*Vitis vinifera* L.) and chestnut (*Castanea* spp.) to achieve 100% survival after transfer from *in vitro* to *ex vitro* (Gonçalves et al., 1998; Carvalho et al., 2001, 2002; Carvalho and Amâncio, 2002a, b). An exhaustive study of grapevine plants subjected to these protocols enabled us to obtain evidence that transfer to high light triggers the expression of a set of specific antioxidative enzymes at the mRNA level, with a marked peak at d2 of *ex vitro* growth (Carvalho et al., 2006). This experimental system was applied in parallel to *Arabidopsis* with the final purpose of over-expressing the genes with interesting expression patterns in both species. *Arabidopsis thaliana*, with its full genome sequenced and transcripts mostly annotated, is a good candidate for gene expression studies, justifying its inclusion. However, the phenotypic characteristics and the results obtained with an oxidative stress gene array pointed to responses much less specific in *Arabidopsis* than in grapevine.

In consequence, and keeping in mind the powerful technologies for functional genomics developed for other species, the first approach of the present research was to characterize the response to photooxidative stress of two important species, *Solanum lycopersicon* and *Nicotiana benthamiana*. The second objective was to compare the responses of both species with others already studied. For the proposed objectives, we propagated and transferred plants of *S. lycopersicon* and *N. benthamiana* to a light intensity four-fold higher than *in vitro*, using the same biochemical and molecular markers found more relevant in previous studies. Unlike *A. thaliana*, *S. lycopersicon* and *N. benthamiana* showed distinct but well-defined patterns of response, with *N. benthamiana* falling closer to the bimodal response of *V. vinifera*, showing a peak of oxidative stress and activation of the antioxidative response system at d2 and a second peak after 7 d of *ex vitro* growth.

Materials and methods

Plant material and *in vitro* growth conditions

Establishment of *Arabidopsis thaliana* WT (ecotype Columbia 9) was performed according to Anderson and Wilson (2000). Stock shoot multiplication and root

induction were adapted from Carvalho et al. (2002), and *in vitro* shoots were sub-cultured every 4 weeks. Seeds of *N. benthamiana* L. and *S. lycopersicon* Mill. were germinated *in vitro* for 3 weeks using Murashige and Skoog (1962), MS (Duchefa Biochemie, Haarlem, NL), basal medium. *In vitro* shoots were sub-cultured every 3 weeks into Murashige and Skoog (1962), MS (Duchefa Biochemie, Haarlem, NL), basal medium supplemented with 0.5 μM α-naphthaleneacetic acid (NAA) and 2.0 μM benzylaminopurine (BAP) in the case of *N. benthamiana*, while *S. lycopersicon* shoots had a supplement of BAP 4.5 μM. Before root induction shoots were elongated in MS supplemented with BAP at 1.67 μM, for 2 weeks. For root induction, explants from the elongation phase received a supplement of 2 μM NAA for 5 d. Cultures were maintained in a growth chamber under light from cool-white fluorescent lamps at a photosynthetic photon flux density (PPFD) of $45 \pm 5\ \mu mol\ m^{-2}\ s^{-1}$ and a photoperiod of 16/8 h. Temperature was $25 \pm 1\ ^{\circ}C$ during the light and $22 \pm 1\ ^{\circ}C$ during the dark.

Ex vitro growth and sampling for analyses

After *in vitro* induction, root expression took place *ex vitro*. Micro-cuttings were transplanted to 6 cm diameter pots containing a sterilized mixture of hydrated peat and perlite (1:1, v/v) and placed in glass chambers (500E, Aralab, Porto Salvo, PT) of 450 L volume. Light was provided by fluorescent lamps Gro-Lux F18W/GRO and, at plant level, PPFD was $200 \pm 10\ \mu mol\ m^{-2}\ s^{-1}$ and the photoperiod was 16/8 h. The programmed relative humidity (RH) inside the glass chamber (98%) was obtained by an ultrasonic fog system controlled by a hygrometer. Temperature was kept at $25 \pm 2\ ^{\circ}C$ during the light and $22 \pm 1\ ^{\circ}C$ during the dark.

The analyses were performed in samples of leaves formed *in vitro* (persistent leaves, referred as PL) at time zero of *ex vitro* growth (d0) and daily during 7 d (d1–7), collected in the middle of the light period.

ROS imaging

Leaves were detached from plants from d0 to d7 of *ex vitro* growth in a 2 mM EDTA solution pH 5.5, and infiltrated in 5 mM 3,3′-diaminobenzidine (DAB) at pH 3.8 to detect hydrogen peroxide (H_2O_2) or in 6 mM nitroblue tetrazolium (NBT) to detect superoxide radical ($O_2^{\cdot-}$) after which they were cleared in 80% ethanol at 60 °C, to remove chlorophyll (Fryer et al., 2002). Images were taken with a digital camera. Incubation in ROS-specific dyes was performed by infiltration through the petiole or by immersion in order to accentuate the colouring of epidermal cells and stomata.

Chlorophyll determination

Chlorophyll was extracted daily from four leaf discs (total area 113 mm^2). Discs were incubated in 3 mL DMSO at 65 °C for 1 h, and absorbance was measured at 645 and 663 nm (adapted from Hiscox and Israelstam, 1979).

The chlorophyll concentration of the extracts was calculated using the equations described by Porra et al. (1989): Chl*a* ($\mu g\ mL^{-1}$) = $12.00 \times A_{663} - 3.11 \times A_{645}$; Chl*b* ($\mu g\ mL^{-1}$) = $20.78 \times A_{645} - 4.88 \times A_{663}$; tot Chl ($\mu g\ mL^{-1}$) = $17.67 \times A_{645} + 7.12 \times A_{663}$; and converted to mg Chl cm^{-2} leaf area (Richardson et al., 2002).

Enzyme activity

Leaf material (0.5 g) was randomly collected daily, frozen in liquid N_2 and stored at 80 °C. Leaves were ground in the presence of liquid N_2 using mortar and pestle, and 50% (w/w) polyvinylpolypyrrolidone was added, as well as 0.2 mM phenylmethylsulphonylfluoride, and 5 mL of ice-cold Tris–HCl buffer, 350 mM, pH 8.0, supplemented with 20 mM sodium ethylenediaminetetraacetate, 11 mM sodium diethyldithiocarbamate (EDTA) and 15 mM cysteine. Homogenates were centrifuged at 27,000*g* for 10 min at 4 °C.

The supernatants, desalted through PD-10 columns (Amersham Pharmacia Biotech, Little Chalfont, UK), were used for all the determinations. Protein concentration was determined according to Bradford (1976), using a commercial kit (Bio-Rad, Hercules, CA).

Native PAGE and activity staining

Isoforms of SOD, CAT and APX were separated using non-denaturing polyacrylamide gels by the procedure of Laemmli (1970). Equal amounts of protein extracts (17 μg for SOD and 4 μg for CAT and APX) were loaded on 7% (CAT) or 10% (SOD and APX) polyacrylamide gels.

For SOD, the gel was stained according to Rao et al. (1996). Gels were incubated for 30 min in 50 mM potassium phosphate buffer (pH 7.8) containing 1 mM EDTA. To identify KCN- and H_2O_2-sensitive isoforms, the incubation solution contained 3 mM KCN or 5 mM H_2O_2, respectively. KCN inhibits Cu-ZnSOD while both Cu-ZnSOD and ISOD are sensitive to H_2O_2, allowing the discrimination of MnSOD. This step was followed by an incubation in 50 mM potassium phosphate buffer (pH 7.8) containing 0.245 mM NBT, 33.2 μM riboflavin and 0.2% tetramethyl ethylene diamine (TEMED) in darkness for 30 min before illumination to visualize SOD isoforms or bands (Donahue et al., 1997).

To visualize CAT profile, gels were stained by the procedure of Anderson et al. (1995). The gels were incubated in 3.27 mM H_2O_2 for 25 min, rinsed in distilled water and then stained in a solution containing 1% (w/v) potassium ferricyanide and 1% (w/v) ferric chloride.

Isoforms of APX were visualized by incubating the gels for 30 min in 50 mM potassium phosphate buffer (pH 7.0) containing 2 mM ascorbate, followed by a 20 min incubation in the same buffer containing 4 mM ascorbate and 2 mM H_2O_2. Finally, gels were stained in 50 mM potassium phosphate buffer, pH 7.8, containing 28 mM TEMED and 2.45 mM NBT for 15 min. Relative quantification of all isoenzyme activities was determined using the software Quantity One (Bio-Rad, Hercules, CA) in comparison to control (d0 = 100%).

RNA isolation and cDNA preparation

Total RNA from leaves was extracted using a commercial kit, RNeasy Plant Mini Kit (Qiagen, Cambridge, MA). RNA samples were treated with RQ1 RNase-Free DNase (Promega, Madison, WI) and reverse transcribed using random hexamers and Superscript II RNase H-reverse transcriptase (Invitrogen, Carlsbad, CA) according to the manufacturer's recommendations.

Real-time PCR and quantification of mRNA levels

Primer pairs used for amplification of all the genes studied are presented in Table 1. The genomic sequences used were from *A. thaliana*. Real-time PCR was performed in 20 μL of reaction mixture composed of cDNA, 0.5 μM gene-specific primers and master mix iQ SYBR Green Supermix (Bio-Rad, Hercules, CA) using an iQ5 Real-Time PCR (Bio-Rad, Hercules, CA). Amplification of PCR products was monitored via intercalation of SYBR-Green (included in the master mix). The following program was applied: initial polymerase activation, 95 °C, 3 min; then 40 cycles at 95 °C, 15 s (denaturation), 57 °C, 30 s (annealing), 72 °C, 20 s (extension) with a single fluorescence reading taken at the end of each cycle. Each run was completed with a melting curve analysis to confirm the specificity of amplification and confirm the lack of primer dimmers. Further, RT-PCR products were resolved on 2% (w/v) agarose gels, run at 4 V cm^{-1} in Tris–acetate–EDTA buffer, along with a 50-bp DNA-standard ladder (Invitrogen GmbH) to confirm the existence of a single product of the desired length. Some of these products were randomly chosen for cloning, using pMOS*Blue* Blunt Ended Cloning Kit (GE Healthcare, Lifesciences), and sequencing in order to confirm their identity.

To generate a baseline-subtracted plot of the logarithmic increase in fluorescence signal (ΔR_n) versus cycle number, baseline data were collected between cycles 5 and 17. All amplification plots were analysed with an R_n threshold of 0.2 to obtain C_T (threshold cycle) and the data obtained were exported into a MS Excel workbook (Microsoft Inc.). In order to compare data from different PCR runs or cDNA samples, C_T values were normalized to the C_T value of *Act2*, a housekeeping gene expressed at a relatively high and constant level (An et al., 1996). The average C_T value for

Table 1. Primers used for evaluation of mRNA levels of the enzymes studied by real-time PCR

Protein name and intracellular localization	mRNA	Primer	
	GenBank accession	Name	Sequence
APX1, cytosolic	X59600	APX1A	5′-GTCCATTCGGAACAATGAGGTTGAC-3′
		APX1B	5′-GTGGGCACCAGATAAAGCGACAT-3′
APX3, peroxisome	U69138, X98276, X98003	APX3-3A	5′-ATGGCTGCACCGATTGTTGATGCG-3′
		APX3-3B	5′-GAACGAAGAAGAGCACACTCATG-3′
Catalase (CAT), peroxisome	CB259031	CAT-A	5′-ATGGATCCTTACAAGTATCGTC-3′
		CAT-B	5′-GAGGTCACTCACGATGTCTC-3′
Copper–zinc SOD, chloroplast, cytosol	BE038231	Cu-ZnSOD-A	5′-GTCATGCGGGTGACCT-3′
		Cu-ZnSOD-B	5′-AGATTGGCATGTGGTGT-3′
Iron SOD, chloroplast	AY065458	ISOD3-A	5′-GATTGGGATGTTGGGTTCAC-3′
		ISOD3-B	5′-GTCAAAACCTCAACGCCATT-3′
Manganese SOD, mytochondria	At3g10920	MnSOD1-A	5′-CCTTACGATTATGGCGCATT-3′
		MnSOD1-B	5′-CTTCACTGGAAGGAGCAAGG-3′
Dehydroascorbate reductase, cytosol	AY140019, At1g75270	DHAR1-A	5′-TAATGACGGATCCGAGAAGG-3′
		DHAR1-B	5′-CTGGTCAAGCTCTCAGGGAC-3′
Monodehydroascorbate reductase, cytosol, peroxisome	At3g27820	MDHAR-A	5′-GGTGATGTTGTGCACTTTGG-3′
		MDHAR-B	5′-TTTCTGCTGACTCACAACCG-3′
Actin 2	At3g18780	Act2-A	5′-ACCTTGCTGGACGTGACCTTACTGAT-3′
		Act2-B	5′-ATGGAAGAGCTGGTCTTTGAGGTTT-3′

Note: Accession numbers correspond to *Arabidopsis thaliana* sequences.

Act2 was 24.94 ($\pm$0.44) for *N. benthamiana* and 25.51 ($\pm$0.39) for *S.lycopersicon* in all plates/templates measured in this series of experiments. Gene expression was calculated using the $\Delta\Delta C_T$ method. Results are presented as fold variation in relation to control (d0).

Statistics

Each treatment was performed twice. All the determinations were obtained with randomly chosen plants. For chlorophyll content and enzyme activities, four independent samples were measured in triplicate ($n = 4$). For real-time PCR, three independent measures were made for each time point ($n = 3$). The results were statistically evaluated through variance analysis comparing the days. Significant values were discriminated with Tukey's post-test, $p < 0.01$, using GraphPad InStat (GraphPad Software, CA). Data are presented $\pm$ standard error (SE).

Results

Plant growth and chlorophyll content

Micropropagated plants of *A. thaliana*, *N. benthamiana* L. and *S. lycopersicon* Mill (tomato) transferred to acclimatization under 200 μmol $m^{-2} s^{-1}$ irradiance (four-fold higher than *in vitro*) were monitored for 7 d, and their morphological and anatomical traits are shown in Figure 1. Unlike *N. benthamiana* and tomato, the pattern of *in vitro* Arabidopsis was not homogeneous. While ca. 60% of the plantlets fared well (Figure 1(G)), the others evidenced severe symptoms of vitrification (Figure 1(H)). In order to compare their behaviour with the other two species, only plants as shown in Figure 1(G) were transferred to *ex vitro*.

The most marked phenotypical difference between *ex vitro N. benthamiana* and tomato is put in evidence in Figure 1. It is possible to distinguish roots in tomato from d2 (Figure 1(A), d2; C and F), while in *N. benthamiana* roots are only present in all plants at d6 (Figure 1(B),d6; D and E). New leaves were not observed in either of the species during the period of analysis.

In tomato, chlorophyll concentration in leaves formed *in vitro*, PL, was ca. twice as high as that of *A. thaliana* and *N. benthamiana* (Figure 2), while the a/b ratio attained higher values in the latter (average between d0 and d7 of 3.5 against 3.0 in tomato and ca. 2.0 in *A. thaliana*) (Figure 2, insets).

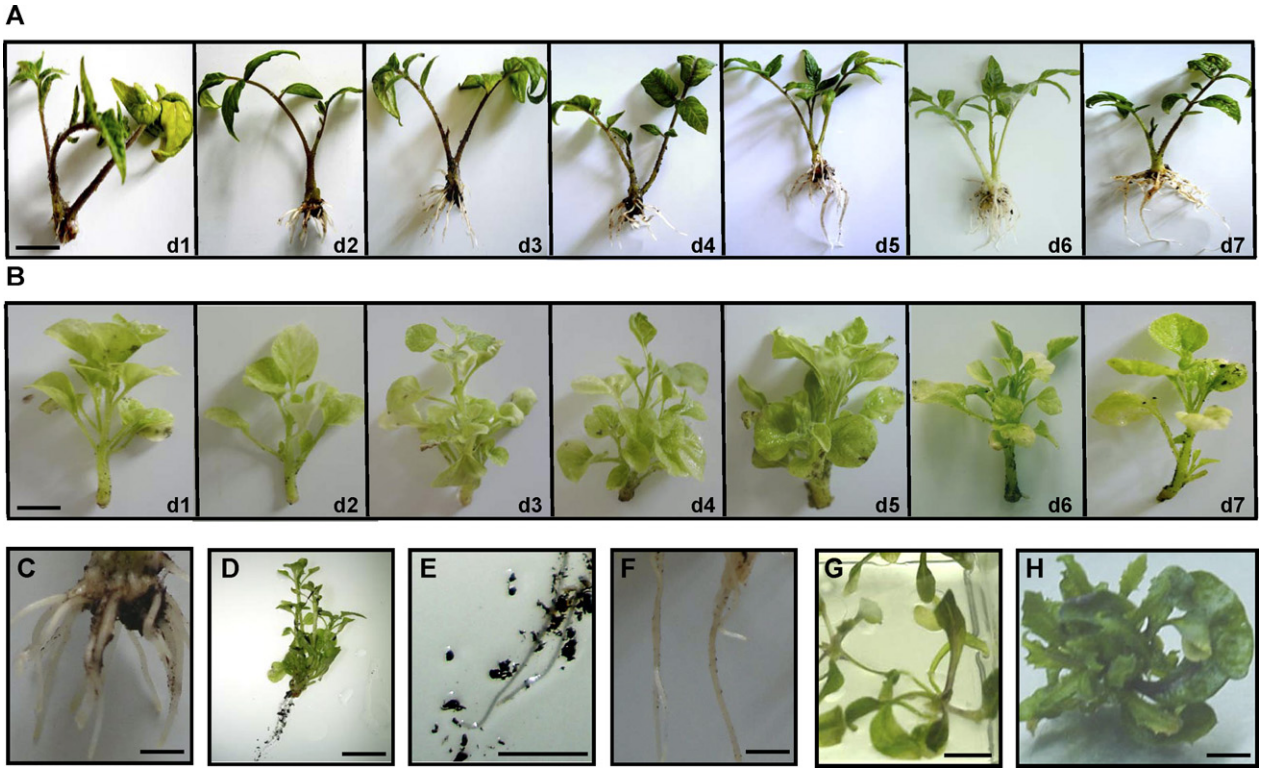

Figure 1. Monitoring the morphology and anatomy of *S. lycopersicon* (A) and of *N. benthamiana* (B) plants during the first 7 d after transfer to *ex vitro* conditions. Plants are subjected to a PPFD of 200 $\pm$ 10 μmol $m^{-2} s^{-1}$, a photoperiod of 16/8 h and a programmed relative humidity (RH) of 98%. Roots are visible in tomato from d2; (C) and (F) show the details of a root on d7. In *N. benthamiana* plants roots are present from d6; (D) and (E) show the details of a root. For comparison, a normal *Arabidopsis thaliana* plantlet (G) and a plantlet evidencing symptoms of vitrification (H), at transfer to *ex vitro* (d0). Bar = 1 cm except (C) and (F) where bar = 0.25 cm.

Detection of ROS

Figures 3 and 4 represent the accumulation of O_2^- and H_2O_2, respectively, in Arabidopsis, tomato and *N. benthamiana* PL, during 7 d after transfer to *ex vitro*. Leaves were collected, infiltrated with NBT for O_2^- or DAB for H_2O_2 depiction and cleared in ethanol, following the procedure described in Materials and methods.

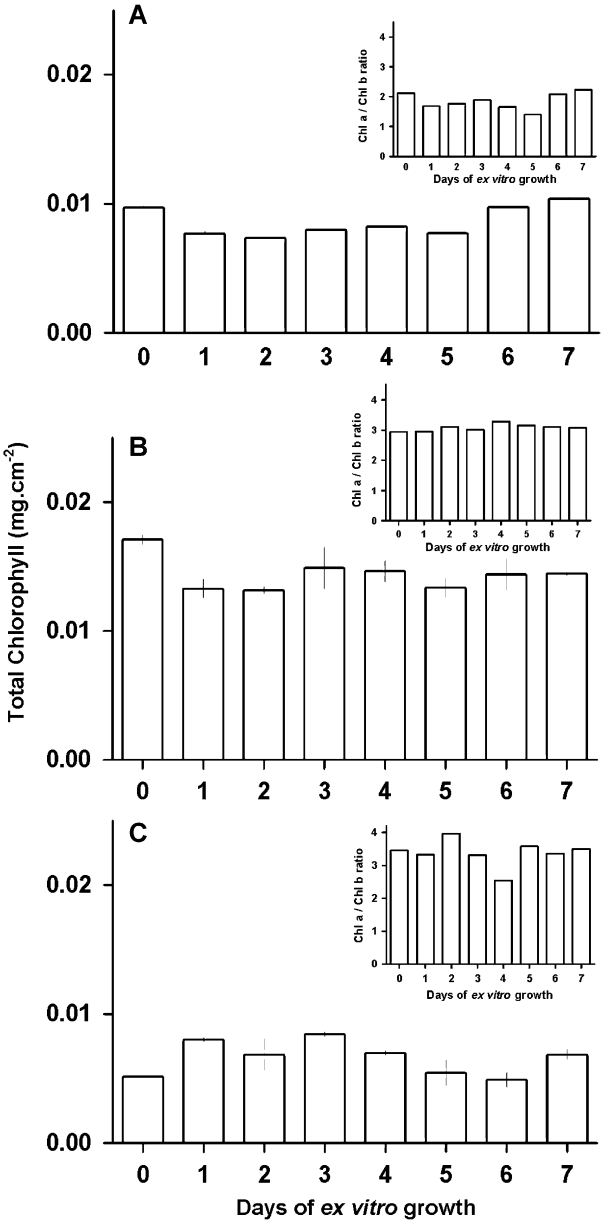

Figure 2. Chlorophyll concentration in leaves of *Arabidopsis thaliana* (A), *S. lycopersicon* (B) and *N. benthamiana* (C) during 7 d after transfer to *ex vitro* conditions. Chlorophyll *a*/chlorophyll *b* ratio is indicated in the inset. Each value is the mean of four replicates (bars indicate standard error).

Imaging of purple formazan deposits (Figure 3), which result from the reaction of NBT with O_2^-, identifies the regions where this ROS molecule is accumulated. The distribution of formazan deposits is uniform throughout the leaf blade but is emphasized in veins. There is an enhanced accumulation of O_2^- on d3 and d6 in tomato and on d2 and d5 in *N. benthamiana*, revealing a similar bimodal pattern in both species, with a 1-day delay in tomato. In Arabidopsis, vein network became progressively coloured and a strong accumulation of O_2^- was visible from d3 to d7 at the whole-leaf level.

The production of H_2O_2 (Figure 4) was imaged in leaves infiltrated with DAB, through its reaction with H_2O_2 in the presence of tissue peroxidases, which produce a brown polymerization product. The leaf accumulation of H_2O_2 in Arabidopsis was more evident on d2–4 and d7. Tomato revealed an evident bimodal pattern, with a high accumulation of deposits on d1 and from d5 on. In *N. benthamiana*, the pattern was less regular than in tomato, with deposits evident on d1–2, d5 and d7.

Anti-oxidative response at the level of enzyme activity and gene expression

To further analyze the effects of transferring *in vitro* Arabidopsis, tomato and *N. benthamiana* to an *ex vitro* environment under high light, we assessed the functioning of the antioxidant system during the first week of *ex vitro* growth. The expression of cDNA sequences from key genes encoding ROS-scavenging and antioxidant enzymes quantified by real-time RT-PCR (see Materials and methods) are shown in Figure 6. In parallel, activities of the isoforms of the respective enzymes were determined in tomato and *N. benthamiana* by activity staining in non-denaturing polyacrylamide gels, the band intensity at each time point corresponding to the comparison with the control (d0 = 100%) (Figure 5). In Arabidopsis, total enzyme activity was quantified spectrophotometrically (Table 2).

In tomato it was possible to distinguish three isoforms of APX, two constitutive and up-regulated in the second half of the experiment (APX-A and APX-B) and one repressed (APX-C), from d2 onwards (Figure 5(A)). From the relative positions of the bands and by comparison with Arabidopsis isozymes (e.g. Panchuk et al., 2002), it was deduced that APX-C corresponds to the cytosolic APX1. In *N. benthamiana*, on the other hand, only two isoforms (APX-D and APX-E) were present,

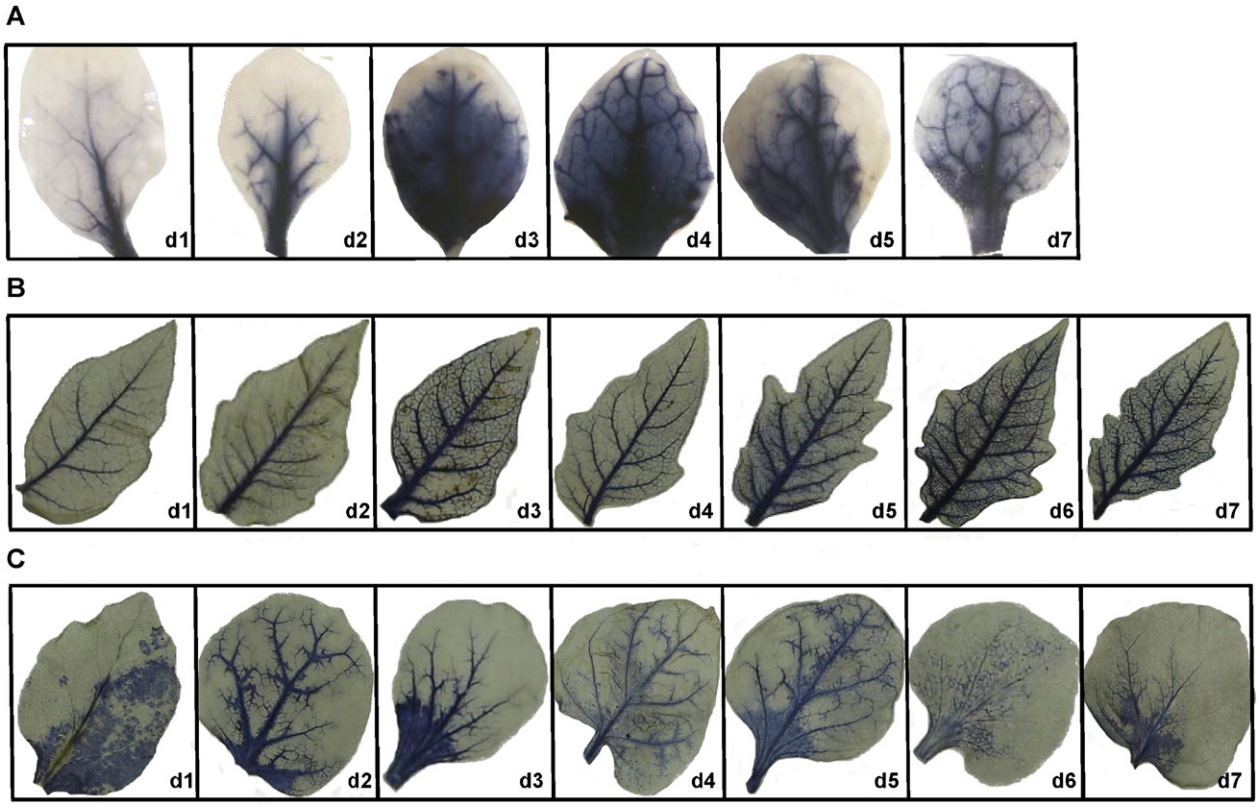

Figure 3. Imaging of superoxide radical accumulation in leaves of *Arabidopsis thaliana* (A), *S. lycopersicon* (B) and *N. benthamiana* (C) during the first 7 d after transfer to *ex vitro* conditions. Incubation in O_2^--specific dye (nitroblue tetrazolium, NBT) was performed by infiltration through the petiole or by immersion in order to accentuate the colouring of epidermal cells and stomata. Images were taken with a digital camera. Amplification: (A) = 5 ×, (B, C) = 3 ×.

both constitutive and without noticeable variation (Figure 5(D)).

The three SOD isoforms present in tomato correspond to MnSODs, as determined through treatment with inhibitors (Figure 5(B)). All isoforms were present after incubation of the gels with H_2O_2 or KCN (for details, see Material and methods), whereas in *N. benthamiana* one of the isoforms disappeared after incubation with H_2O_2, thus corresponding to an ISOD (Figure 5(E)). From the three MnSODS present in tomato, the constitutive MSOD-A and B were slightly down-regulated all along the experiment while MSOD-C disappeared after d2.

After activity staining for CAT, two constitutive isoforms (CAT-A and CAT-B) in tomato (Figure 5(C)) and one isoform in *N. benthamiana* (Figure 5(F)) were detected. CAT-A decreased in the second half of the experiment while CAT-B peaked on d2. In *N. benthamiana,* CAT activity was maximum on d1.

In Arabidopsis, the activity of APX, CAT and SOD (Table 2) showed the highest values on d1 but without a defined peak of activity, except in the case of APX. At the gene expression level, the antioxidative system response was absolutely not significant (Figure 6(A)).

Concerning *S. lycopersicon* and *N. benthamiana*, the timing of up-regulation of antioxidative genes after transfer to *ex vitro* differed between the two species. In tomato some transcripts increased in the order of 100 or 200 times, immediately after the onset of high light (d1), declining thereafter, while *N. benthamiana* showed a bimodal pattern of transcript expression with peaks measured between 10- and 30-fold variation at d2 and d7 (Figure 6). With reference to APX transcripts, *N. benthamiana APX3* increased significantly on d2 and d7 and *APX1* showed significant changes (nine-fold increase) on d7. In tomato, only *APX3* was moderately up-regulated on d1.

Transcript expression of tomato *MSOD* and *ISOD* was high on d1 (Figure 6), unlike *Cu-ZnSOD*, which increased only slightly. In *N. benthamiana*, the three transcript isoforms presented the characteristic bimodal variation, *ISOD* showing the highest abundance. In tomato, *CAT* showed a

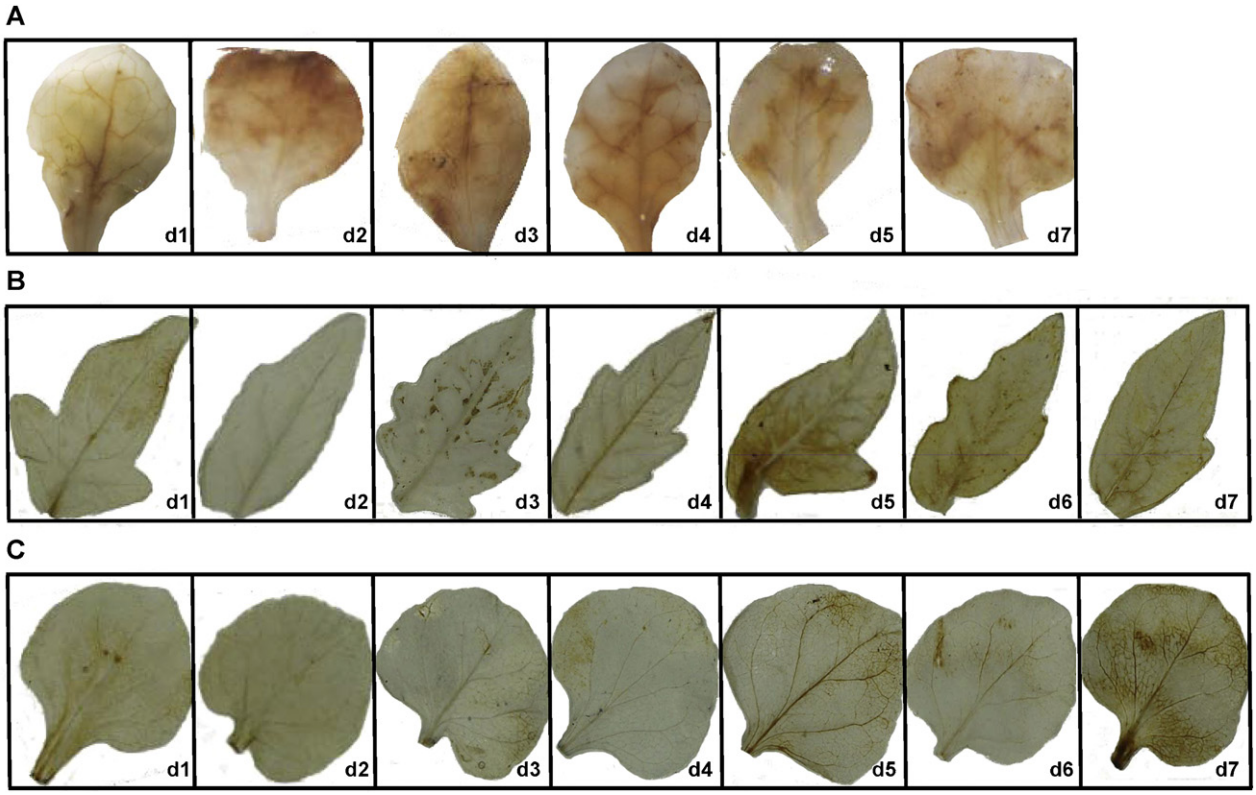

Figure 4. Imaging of hydrogen peroxide accumulation in leaves of *Arabidopsis thaliana* (A), *S. lycopersicon* (B) and *N. benthamiana* (C) during the first 7 d after transfer to *ex vitro* conditions. Incubation in H_2O_2-specific dye (3,3′-diaminobenzidine, DAB) was performed by infiltration through the petiole. Images were taken with a digital camera. Amplification: (A) = 5×, (B, C) = 3×.

significant up-regulation on d1 (Figure 6), while in *N. benthamiana CAT* showed the same pattern as the APX and SOD transcripts, with a peak on d2 (25-fold) and a smaller one on d7 (seven-fold).

Tomato *DHAR* and *MDHAR* transcripts followed the pattern of up-regulation on d1, while in *N. benthamiana* the abundance of both transcripts was once more bimodal, with peaks on d2 and d7 (Figure 6).

The uncertain results reported here for Arabidopsis together with others collected from an array of *A. thaliana* oxidative stress genes (data not shown) point to unspecific responses from this species under the present experimental conditions. It is possible that *in vitro* growth induced drastic modifications in Arabidopsis development and did not allow the detection of clear changes in the expression of interesting stress response genes. Therefore, we decided not to extend further the comparison of the other two species with Arabidopsis, instead comparing them with each other and, when necessary, discussing in association with previous results obtained for grapevine (Carvalho et al., 2006).

Discussion

S. lycopersicon and *N. benthamiana* transferred from *in vitro* to *ex vitro* yielded 100% survival when the experiment was prolonged to d28. Previously, our rooting methodology led to positive results in species recalcitrant to root, such as *Castanea* spp. and *V. vinifera* L. (Carvalho and Amâncio, 2002a; Carvalho et al., 2002; Vatulescu et al., 2004). It consists of *in vitro* auxin induction for a short period (4–5 d) and then transplantation to *ex vitro*, so that root protrusion and elongation takes place entirely *ex vitro*. This reduces the time of plant production and promotes the formation of a more adjusted and functional root system (McClelland et al., 1990). Here, the two species under scrutiny achieved rooting results through different strategies. Tomato plants showed a very positive response; roots protruding and elongating from d2 were organized in a robust root system by d7. This rhizogenic behaviour may explain the expansion of new leaves from d7 (data not shown). *N. benthamiana*, conversely, began expanding roots only on d6, which resulted in a delay of new leaf production.

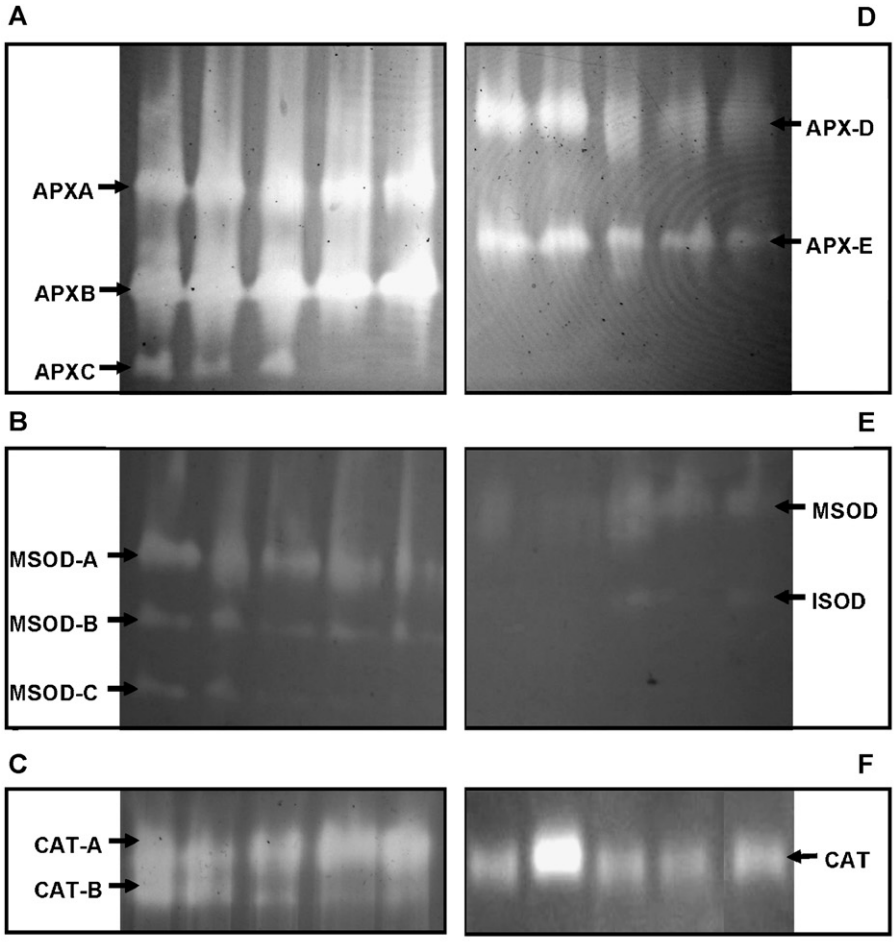

	d0	d1	d2	d4	d7
APX-A	100	99	98	129	132
APX-B	100	105	106	123	121
APX-C	100	97	96		
MSOD-A	100	93	86	83	81
MSOD-B	100	88	80	79	80
MSOD-C	100	93	85		
CAT-A	100	107	101	83	76
CAT-B	100	104	125	116	114

d0	d1	d2	d4	d7	
100	97	93	95	98	APX-D
100	104	103	100	91	APX-E
100	108	115	128	145	ISOD
100	104	117	133	148	MSOD
100	254	90	69	107	CAT

Figure 5. APX (A, D), SOD (B, E) and CAT (C, F) isoenzyme in gel activities of leaves of *S. lycopersicon* (A, B, C) and *N. benthamiana* (D, E, F) plants during the 7 d of *ex vitro* growth. Total protein extracts were subjected to native PAGE followed by activity staining for each of the three enzymes. APX isoforms were identified by comparison with Arabidopsis molecular mass profile. Discrimination between SOD isoforms was revealed by inhibition with KCN and H_2O_2. Relative quantification of the isoenzymes' activities in relation to d0 (d0 = 100%) using the software Quantity One (Bio-Rad, Hercules, CA).

Total chlorophyll content of sun plants normally shows a direct relationship to the light intensity reaching the plants; therefore, it increases after transfer to *ex vitro* growth (Carvalho et al., 2002; Pospíšilová et al., 2000; van Huylenbroek et al., 1998). In opposition to these reports where chlorophyll determinations were performed every 7 d, in the present study chlorophyll was analysed daily during the first 7 d *ex vitro*. This thorough analysis revealed that, in *N. benthamiana* total

Table 2. Specific enzyme activity of superoxide dismutase, ascorbate peroxidase and catalase in extracts of *Arabidopsis thaliana* from day 0 to day 7 of *ex vitro* growth

	d0	d1	d2	d4	d7
APX (μmol AsA oxidized min^{-1} mg $prot^{-1}$)	1.68b	3.08c	1.79b	0.78a	0.85a
SOD (units mg $prot^{-1}$)	0.44b	0.59c	0.29a	0.46b	0.28a
CAT (units mg $prot^{-1}$)	0.38a	0.65c	0.56bc	0.50b	0.39a

Note: Mean comparison in rows. Values in each row followed by different letters (a, b, c) are significantly different, $p < 0.005$, $n = 4$.

chlorophyll is one half that of tomato, the former raising for the first 3 d *ex vitro* and the latter decreasing immediately after transfer. In both species, the chl *a*/chl *b* ratio matched well with values typical of field-grown leaves.

In general, environmental stresses imposed to plants are thought to be mediated by oxidative stress due to the production of ROS (Bartosz, 1997). To have an insight into ROS production and accumulation due to light stress after transfer of plants to *ex vitro* under irradiances four-fold higher, leaves of both species were analysed by imaging techniques for H_2O_2 and O_2^- visualization. Apparently, the decrease in chlorophyll content in tomato is not synonymous of a lower capacity to recover from the photooxidative stress imposed at transfer to *ex vitro*. Imaging results put in evidence an early accumulation of ROS:H_2O_2 on d1 in tomato and on d2 in *N. benthamiana*, O_2^- showing peaks on d2 in *N. benthamiana* and on d3 in tomato. This pattern confirms photooxidative stress caused by transfer to *ex vitro* as described by van Huylenbroek et al. (2000) and Carvalho et al. (2001) and matches results obtained in grapevine under the same experimental conditions, either O_2^- and H_2O_2 imaging (Vilela et al., 2007) or H_2O_2 concentrations (Carvalho et al., 2006). Thereafter, recovery from photooxidative stress explains the decrease of accumulation of both ROS. A second, although less intense, production of the same ROS was visible in *N. benthamiana* on d5–6 and *S. lycopersicon* on d6–7, at first for O_2^-, and 24 h later for H_2O_2. A bimodal production of H_2O_2 was described in grapevine (Carvalho et al., 2006), the second peak being assigned to ontogenic formation of new structures. Observing the pattern of ROS distribution, O_2^- is uniformly distributed throughout the leaf blade while H_2O_2 is mainly present in veins, under a pattern similar to grapevine (Vilela et al., 2007). This preferential accumulation of H_2O_2 points to its role as a signalling molecule. In contrast with O_2^-, which has a short half-life and is unable of crossing biological membranes, H_2O_2 diffusion over relatively long distances between cells (Vranová et al., 2002; Mullineaux et al., 2006) enables its role as a central player in the signalling of several plant processes (Mittler et al., 2004).

It is described for several plant species that the activities of some antioxidant enzymes increase upon exposure to photooxidative stress, e.g. *A. thaliana* DHAR activity was enhanced following an increase in irradiance (Kubo et al., 1999); in leaves of tobacco transferred to an higher irradiance (380 μmol $m^{-2}s^{-1}$) the activities of asc–glut cycle enzymes, including GR, increased simultaneously with ROS production (Kadleček et al., 2003); in grapevine transferred from 50 to 200 μmol $m^{-2}s^{-1}$, CAT, SOD and asc–glut cycle enzyme activities also increased, with the exception of GR (Carvalho et al., 2006). The asc–glut cycle is present in practically every cellular compartment (Mittler et al., 2004), which, together with the high affinity of APX to H_2O_2, suggests the crucial role of this cycle in the control of ROS in different cell compartments. CAT, on the other hand, with its lower affinity to H_2O_2 and being present mainly in peroxisomes, is associated with the processing of H_2O_2 generated in photorespiration (Vandenabeele et al., 2004), although it is also important in cases of excessive H_2O_2 formation, as in strong oxidative stress (Mittler, 2002). APX1 is the cytosolic isoform of APX and its expression is induced by light (Karpinski et al., 1997). In tomato, constitutive isoforms of APX were active at the moment of transfer, indicating that more likely due to photooxidative stress than to light activation, enzyme activity was up-regulated. APX1 is critical in the control of the signalling role of H_2O_2, its major subcellular localization in the cytosol is described as relevant for communicating the information to the nucleus (Shigeoka et al., 2002; Mullineaux et al., 2006), thus regulating the molecular mechanisms of tolerance against oxidative stress. It is then relevant to notice that H_2O_2 accumulation, high on d1, decreased while APX1 was present. Conversely, in *N. benthamiana*, APX activity was detected during the whole experiment. It is interesting to point out that, in tomato, *APX1* and *APX3* transcript abundance remained close to basal levels, indicating that the enzyme present on d0 was enough to sustain the increase in activity observed.

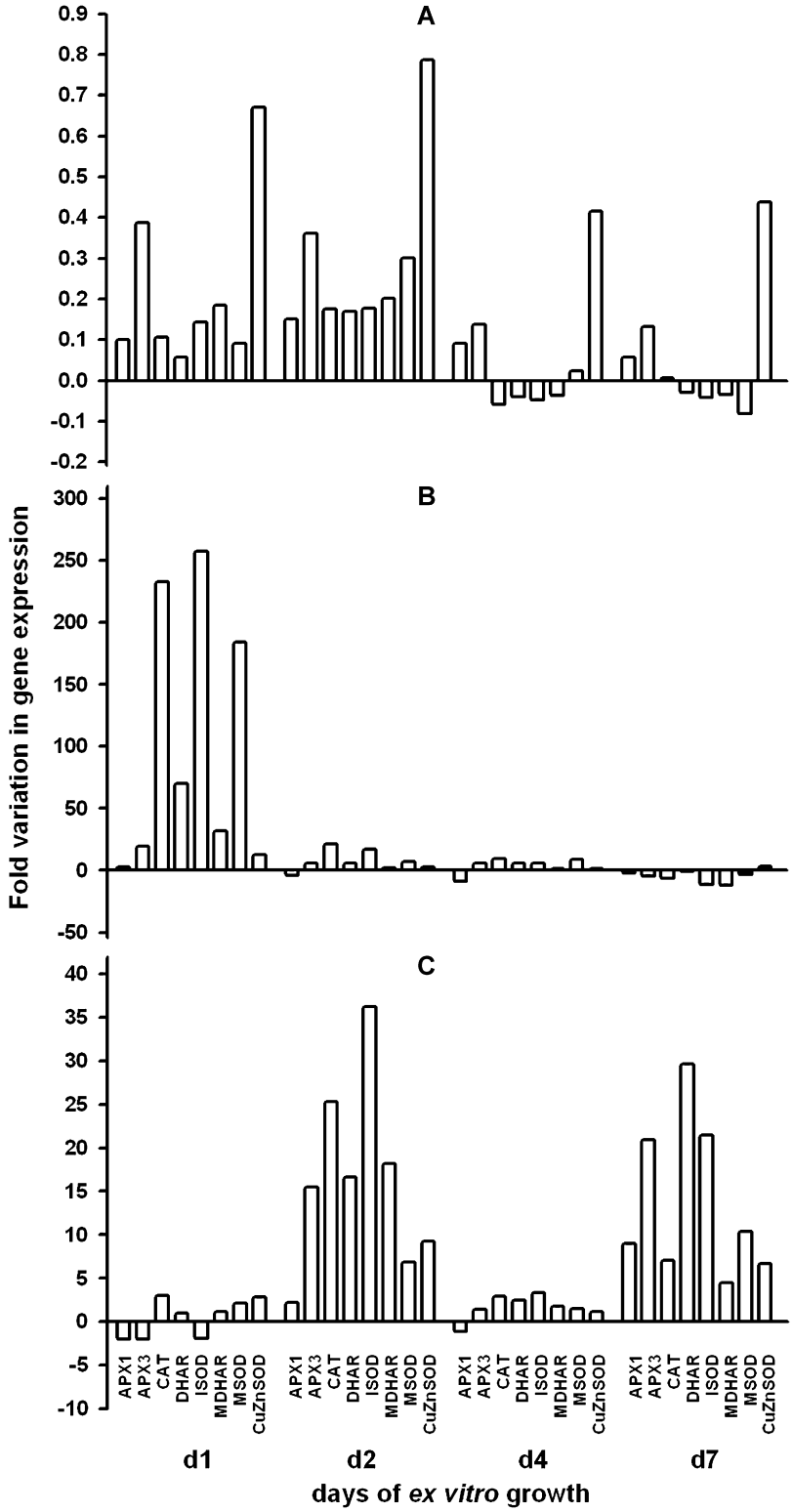

Figure 6. Changes in the expression levels of genes of the antioxidative system. Quantification of mRNA levels of those *Arabidopsis thaliana* (A), *S. lycopersicon* (B) and *N. benthamiana* (C) genes was performed during the first week of *ex vitro* growth. mRNA was isolated from leaves, converted to cDNA and subjected to real-time PCR. Relative amounts were calculated and normalized with respect to *Act2* mRNA. Each time point is compared with d0 leaves ($n = 3$). For clarity purposes, three different scales were used.

Roots can be observed from d2 in tomato and new leaves begin expanding after d7 of transfer to *ex vitro* (data not shown), whereas in *N. benthamiana*, roots are visible later, by d6, and new leaves begin expanding after that (data not shown). Together with these ontogenic events and the previously referred ROS accumulation, transcript abundance of all the genes monitored increased by several fold on d7, in *N. benthamiana*. This is consistent with the "peak on day 6" reported in grapevine, which was not associated with oxidative stress but with the formation of new structures (Carvalho et al., 2006). In tomato, however, roots protrude very early, unconnected in time from leaf expansion, which can explain the absence of a second peak of transcript expression.

Considering the growth and survival of the plants, the protocol applied resulted in a positive response of both tomato and *N. benthamiana*, enabling the production of sturdy, healthy plants after 28 d of *ex vitro* growth. Additionally, both species increased the H_2O_2 pool and activated an antioxidant response at the level of gene expression after transfer to *ex vitro* under high light. This general response was common to both species and falls into the pattern already described for other plant species (van Huylenbroek et al., 2000; Carvalho et al., 2006). Finally, taking a closer look at the mechanism and timing of the response, it is clear that the species under study used different strategies to overcome the initial period of light stress. In tomato, key genes of antioxidative response were up-regulated immediately after exposure to HL, coinciding with the generation of $O_2^{\cdot-}$ and H_2O_2, promptly processed. The protrusion of roots immediately after the antioxidative response, separated in time from the expansion of new leaves, avoided the increase in gene expression related to these ontogenic events (Carvalho et al., 2006). *N. benthamiana* displayed a typical bimodal pattern, with a peak of expression of key genes of antioxidative response on d2, correlating with the generation of ROS and a second peak on d7, indicating a signalling for the simultaneous formation of new structures, roots and new leaves.

In conclusion, the behaviour of *N. benthamiana* falls closely into the pattern already reported for grapevine (Carvalho and Amâncio, 2002a; Carvalho et al., 2006), rendering this species under the described experimental protocol a suitable model for molecular analysis of photooxidative stress in grapevine.

Acknowledgements

The research was funded by Plurianual funds to CBAA and Fundação para a Ciência e Tecnologia, with the post-doc grant SFRH/BPD/5707/2001 to L.C.C. and the project POCTI/AGG/37968/2001 that includes a research grant to B.J.V.

References

An Y-Q, McDowell JM, Huang S, McKinney EC, Chambliss S, Meagher RB. Strong, constitutive expression of the *Arabidopsis* ACT2/ACT8 actin subclass in vegetative tissues. Plant J 1996;10:107–21.

Anderson M, Wilson F. Growth, maintenance, and *Arabidopsis* genetics resources. In: Zoe A. Wilson, editor. *Arabidopsis* A Practical Approach. Oxford: Oxford University Press; 2000. p. 1–28.

Anderson MD, Prasad TK, Stewart CR. Changes in isozyme profiles of catalase, peroxidase and glutathione reductase during acclimation to chilling in mesocotyls of maize seedlings. Plant Physiol 1995;109:1247–57.

Appel K, Hirt H. Reactive oxygen species: metabolism, oxidative stress, and signal transduction. Annu Rev Plant Biol 2004;55:373–99.

Asada K. The water–water cycle in chloroplasts: scavenging of active oxygens and dissipation of excess photons. Annu Rev Plant Physiol Plant Mol Biol 1999; 50:601–39.

Bartosz G. Oxidative stress in plants. Acta Physiol Plant 1997;19:47–64.

Bradford MM. A rapid and sensitive method for the quantification of microgram quantities of protein utilizing the principle of protein dye binding. Anal Biochem 1976;72:248–54.

Carvalho LC, Osório ML, Chaves MM, Amâncio S. Chlorophyll fluorescence as an indicator of photosynthetic functioning of in vitro grapevine and chestnut plantlets under ex vitro acclimatization. Plant Cell Tissue Organ Cult 2001;67:271–80.

Carvalho L, Amâncio S. Effect of ex vitro conditions on growth and acquisition of autotrophic behaviour during the acclimatization of chestnut regenerated in vitro. Sci Hortic 2002a;95:151–64.

Carvalho LC, Amâncio S. Antioxidant defence system in plantlets transferred from in vitro to *ex vitro*: effects of increasing light intensity and CO_2 concentration. Plant Sci 2002b;162:33–40.

Carvalho LC, Santos P, Amâncio S. Effect of light intensity and CO_2 concentration on growth and the acquisition of in vivo characteristics duringacclimatization of grapevine regenerated in vitro. Vitis 2002;41:1–6.

Carvalho L, Vilela B, Vidigal P, Mullineaux P, Amâncio S. Activation of the ascorbate–glutathione cycle is an early response of micropropagated *Vitis vinifera* L. explants transferred to ex vitro. Int J Plant Sci 2006; 167:739–50.

Chew O, Rudhe C, Glaser E, Whelan J. Characterization of the targeting signal of dual targeted pea glutathione reductase. Plant Mol Biol 2003;53:341–56.

Desjardins Y. Photosynthesis in vitro – on the factors regulating CO_2 assimilation in micropropagation systems. Acta Hortic 1995;393:45–61.

Donahue JL, Okpodu CM, Cramer CL, Grabau EA, Alscher RG. Responses of antioxidants to paraquat in pea leaves. Relationships to resistance. Plant Physiol 1997; 113:249–57.

Fryer MJ, Oxborough K, Mullineaux PM, Baker NR. Imaging of photo-oxidative stress responses in leaves. J Exp Bot 2002;53:1249–54.

Gonçalves JC, Diogo G, Amâncio S. In vitro propagation of chestnut (*Castanea sativa* × *C. crenata*): effects of rooting treatments on plant survival and anatomical changes during adventitious root formation. Sci Hortic 1998;72:265–75.

Hiscox JD, Israelstam GF. A method for the extraction of chlorophyll from leaf tissue without maceration. Can J Bot 1979;57:1332–4.

Kadleček P, Rank B, Tichá I. Photosynthesis and photoprotection in *Nicotiana tabacum* L. in vitro grown plantlets. J Plant Physiol 2003;160:1017–24.

Karpinski S, Escobar, Karpinska B, Creissen G, Mullineaux PM. Photosynthetic electron transport regulates the expression of cytosolic ascorbate peroxidase genes in *Arabidopsis* during excess light stress. Plant Cell 1997;9:627–40.

Kozai T, Smith MAL. Environmental control in plant tissue culture – general introduction and overview. In: Aitken Christie J, Kozai T, Smith ML, editors. Automation and environmental control in plant tissue culture. Dordrecht: Kluwer Academic Publishers; 1995. p. 301–18.

Kubo A, Aono M, Nakajima N, Saji H, Tanaka K, Kondo N. Differential responses in activity of antioxidant enzymes to different environmental stresses in *Arabidopsis thaliana*. J Plant Res 1999;112:279–90.

Kwak JM, Nguyen V, Schroeder JI. The role of reactive oxygen species in hormonal responses. Plant Physiol 2006;141:323–9.

Laemmli UK. Cleavage of structural proteins during the heat of bacteriophage T4. Nature 1970;227:680–5.

McClelland MT, Smith MA, Carothers ZB. The effects of in vitro and ex vitro root initiation on subsequent microcutting root quality in three woody plants. Plant Cell Tissue Organ Cult 1990;23:115–23.

Mittler R. Oxidative stress, antioxidants and stress tolerance. Trends Plant Sci 2002;7:405–10.

Mittler R, Vanderauwera S, Gollery M, Breusegem FV. Reactive oxygen gene network of plants. Trends Plant Sci 2004;9:490–8.

Mullineaux PM, Karpinski S. Signal transduction in response to excess light: getting out of the chloroplast. Curr Opin Plant Biol 2002;5:43–8.

Mullineaux PM, Karpinski S, Baker N. Spatial dependence for hydrogen peroxide-directed signaling in light stressed plants. Plant Physiol 2006;141:346–50.

Murashige T, Skoog F. A revised medium for rapid growth and bio assays with tobacco tissue cultures. Physiol Plant 1962;15:473–97.

Noctor G, Foyer CH. Ascorbate and glutathione: keeping active oxygen under control. Annu Rev Plant Physiol Plant Mol Biol 1998;49:249–79.

Panchuk II, Volkov RA, Schoffl F. Heat stress- and heat shock transcription factor-dependent expression and activity of ascorbate peroxidase in *Arabidopsis*. Plant Physiol 2002;129:838–53.

Porra RJ, Thompson WA, Kriedemann PE. Determination of accurate extinction coefficients and simultaneous equations for assaying chlorophylls *a* and *b* extracted with four different solvents: verification of the concentration of chlorophyll standards by atomic absorption spectrometry. Biochim Biophys Acta 1989;975:384–94.

Pospíšilová J, Haisel D, Synková H, Čatský J, Wilhelmová N, Plzáková Š, Procházková D, Šrámek F. Photosynthetic pigments and gas exchange during ex vitro acclimation of tobacco plantlets as affected by CO_2 supply and abcisic acid. Plant, Cell, Tiss Org Cult 2000;61:125–33.

Rao MV, Paliyath G, Ormrod DP. Ultraviolet-B- and ozone-induced biochemical changes in antioxidant enzymes of *Arabidopsis thaliana*. Plant Physiol 1996;110: 125–36.

Richardson AD, Duigan SP, Berlyn GP. An evaluation of noninvasive methods to estimate foliar chlorophyll content. New Phytol 2002;153:185–94.

Shigeoka S, Ishikawa T, Tamoi M, Miyagawa Y, Takeda T, Yabuta Y, et al. Regulation and function of ascorbate peroxidase isoenzymes. J Exp Bot 2002;53:1305–19.

Torres MA, Jones JDG, Dangl JL. Reactive oxygen species signaling in response to pathogens. Plant Physiol 2006; 141:373–8.

van Huylenbrœk JM, Piqueras A, Debergh PC. Photosynthesis and carbon metabolism in leaves formed prior and during *ex vitro* acclimatization of micropropagated plants. Plant Sci 1998;134:21–30.

van Huylenbroeck JM, Piqueras A, Deberg PC. The evolution of photosynthetic capacity and the antioxidant enzymatic system during acclimatization of micropropagated *Calathea* plants. Plant Sci 2000;135: 59–66.

Vandenabeele S, Vanderauwera S, Vuylsteke M, Rombauta S, Langebartels C, Seidlitz HK, et al. Catalase deficiency drastically affects gene expression induced by high light in *Arabidopsis thaliana*. Plant J 2004; 39:45–58.

Vatulescu AD, Fortunato AS, Sa MC, Amancio S, Ricardo CP, Jackson PA. Cloning and characterisation of a basic IAA oxidase associated with root induction in *Vitis vinifera*. Plant Physiol Biochem 2004;42:609–15.

Vilela BJ, Carvalho LC, Ferreira J, Amâncio S. Imaging of photooxidative stress symptoms and stomatal functioning in *Vitis vinifera* L. transferred from *in vitro* to *ex vitro* under increased light. Plant Cell Rep 2007; DOI:10.1007/s00299-007-0427-3.

Vranová E, Inzé D, van Breusegem F. Signal transduction during oxidative stress. J Exp Bot 2002;53:1227–36.